Transl Clin Pharmacol. 2020 Sep;28(3):147-159
https://doi.org/10.12793/tcp.2020.28.e15
pISSN 2289-0882·eISSN 2383-5427

Translational and Clinical Pharmacology TCP

Original Article

Qualification and application of liquid chromatography-quadrupole time-of-flight mass spectrometric method for the determination of carisbamate in rat plasma and prediction of its human pharmacokinetics using physiologically based pharmacokinetic modeling

Byeong ill Lee, Jeong-hyeon Lim, Min-Ho Park, Seok-Ho Shin, Jin-Ju Byeon, Jang-mi Choi, Seo-jin Park, Min-jae Park, Yuri Park, and Young G. Shin *

College of Pharmacy, Chungnam National University, Daejeon 34134, Korea

Received: Aug 3, 2020
Revised: Sep 14, 2020
Accepted: Sep 17, 2020

***Correspondence to**
Young G. Shin
College of Pharmacy, Chungnam National University, 99 Daehak-ro, Yuseong-gu, Daejeon 34134, Korea.
E-mail: yshin@cnu.ac.kr

ORCID iDs
Young G. Shin
https://orcid.org/0000-0002-7135-8988

Funding
This research was supported by a research fund of the Ministry of Food and Drug Safety (19172MFDS163).

Reviewer
This article was reviewed by peer experts who are not TCP editors.

Conflict of Interest
- Authors: Nothing to declare
- Reviewers: Nothing to declare
- Editors: Nothing to declare

Author Contributions
Conceptualization: Lee BI, Shin YG; Data curation: Lee BI, Lim JH, Park MH, Shin SH, Byeon JJ, Choi JM, Park SJ, Park MJ, Park Y; Formal analysis: Lee BI; Investigation: Lee BI,

ABSTRACT

Carisbamate is an antiepileptic drug and it also has broad neuroprotective activity and anticonvulsant reaction. In this study, a liquid chromatography-quadrupole time-of-flight mass spectrometric (LC-qTOF-MS) method was developed and applied for the determination of carisbamate in rat plasma to support *in vitro* and *in vivo* studies. A quadratic regression (weighted 1/concentration^2), with an equation $y = ax^2 + bx + c$, was used to fit calibration curves over the concentration range from 9.05 to 6,600 ng/mL for carisbamate in rat plasma. Preclinical *in vitro* and *in vivo* studies of carisbamate have been studied through the developed bioanalytical method. Based on these study results, human pharmacokinetic (PK) profile has been predicted using physiologically based pharmacokinetic (PBPK) modeling. The PBPK model was optimized and validated by using the *in vitro* and *in vivo* data. The human PK of carisbamate after oral dosing of 750 mg was simulated by using this validated PBPK model. The human PK parameters and profiles predicted from the validated PBPK model were similar to the clinical data. This PBPK model developed from the preclinical data for carisbamate would be useful for predicting the PK of carisbamate in various clinical settings.

Keywords: Qualification; LC-MS; Carisbamate; PBPK Modeling

INTRODUCTION

Carisbamate (S-2-O-carbamoyl-1-o-chlorophenyl-ethanol) is an investigational neuromodulatory agent, initially developed from SK Biopharmaceuticals (Seongnam, Korea) for antiepileptic treatment [1-6]. Although the exact mechanism of action for carisbamate is not known, carisbamate has been studied for the treatment of epilepsy, essential tremor and migraine [4,5]. In phase I clinical trials to healthy subjects, carisbamate has shown

Lim JH; Methodology: Lee BI, Lim JH, Park MH; Project administration: Lee BI, Shin YG; Resources: Shin YG; Software: Lee BI, Lim JH, Shin SH; Supervision: Shin YG; Validation: Lee BI; Visualization: Lee BI; Writing - original draft: Lee BI; Writing - review & editing: Lim JH, Park MH, Shin SH, Byeon JJ, Choi JM, Park SJ, Park MJ, Park Y, Shin YG.

linear pharmacokinetics at doses of 100 to 1,500 mg, high oral bioavailability (F) of > 95% and a low oral clearance (CL/F) of 3.4–4.2 L/h, equaling < 5% of liver blood flow [1,2,7]. The drug also has shown efficacy and tolerability in a phase II clinical trial for epilepsy patients, and three phase III clinical trials have been completed for treatment in partial seizures [8-10]. Among them, only one phase III clinical trial (randomized double-blind) study showed significant efficacy results in adults with refractory partial seizures receiving a dose of 400 mg/day [11,12]. In 2008, carisbamate was provisionally approved by the Food and Drug Administration for adjunctive treatment for patients aged 16 years or over with partial onset seizures (brand name: comfyde), but failed to receive marketing approval in 2009. Carisbamate is currently undergoing clinical trials for Lennox Gastaut syndrome as an indication by SK Biopharmaceuticals.

Recently, physiologically based pharmacokinetic (PBPK) model has been increasingly used as a powerful tool to predict clinical pharmacokinetic (PK) parameters and profiles by using preclinical Absorption, Distribution, Metabolism, and Excretion (ADME)/PK data [13-20]. PBPK modeling is a very complex mathematical model that reflects systemically specific physiological properties and drug's physicochemical properties [21]. The PBPK model has been applied in the pharmaceutical industry to predict ADME/PK properties of drugs by using *in vitro* and *in vivo* properties as an input data [22-24].

In this study, a simple and robust liquid chromatography-quadrupole time-of-flight mass spectrometric (LC-qTOF-MS) method for carisbamate was developed and successfully applied to *in vitro* and *in vivo* PK studies in rat. Based on these results, a PBPK model was built, optimized and validated for predicting the PK of carisbamate in humans. After establishing the PBPK model, the human PK of carisbamate was predicted and compared with the reference clinical PK data associated with food effect PK studies [7]. To the authors' best knowledge, this is the first approach for human PK prediction of carisbamate through PBPK model. The information in this study will help designing the studies related to various clinical studies of carisbamate.

METHODS

Chemicals and reagents

Carisbamate was purchased from Toronto Research Chemical (Ontario, Canada). Verapamil was purchased from Sigma-Aldrich (St, Louis, MO, USA). Formic acid was purchased from Daejung Chemical (Siheung, Korea). Male Sprague-Dawley (SD) rat and human liver microsomes were purchased from Corning Incorporated (Corning, NY, USA). Acetonitrile (ACN) of HPLC grade was purchased from Honeywell Burdick & Jackson (Ulsan, Korea). Distilled water (DW) of HPLC grade was purchased from Samchun Chemical (Pyeongtaek, Korea). All other chemicals reagents were of analytical grade and purchased from commercial sources.

Preparation of stocks, standard (STD) and quality control (QC) Samples

Stock solution of carisbamate (1 mg/mL) was prepared in dimethyl sulfoxide (DMSO). The sub-stock solution (0.2 mg/mL) was made by diluting the stock solution with DMSO. Seven calibration standard concentrations of carisbamate were prepared by serial dilution of the sub-stock solution with DMSO. The calibration samples were prepared by spiking the diluted calibration standard solutions into blank rat plasma to obtain final plasma concentrations of 9.05, 27.2, 81.3, 244, 733, 2,200 and 6,600 ng/mL. QC samples with

concentrations of 15.04 (low QC), 165.46 (medium QC) and 1,820 (high QC) ng/mL were prepared in the same manner.

The stock solution (1 mg/mL) for the internal standard (ISTD, verapamil) was prepared in DMSO and stored in the refrigerator at −20°C until use. The ISTD was diluted to prepare a final spiking concentration of 20 ng/mL in ACN prior to sample preparation.

Sample preparation

Fourty microliters of the blank rat plasma samples were placed in cluster tubes, and 4 μL of the standard or QC samples was added to each cluster tube, whereas 4 μL of make-up solution (DMSO) was added to each study samples to prepare the same matrix conditions.

The 150 μL of ACN containing ISTD was added to the standard, QC and study samples for protein precipitation. Samples were centrifuged at 10,000 rpm for 5 minutes and then supernatants were evaporated to dryness under vacuum in a Savant SpeedVac™ (Thermo Scientific, Rockford, IL, USA). The dried residues were reconstituted using ACN/DW (1:1), vortexed, and then centrifuged at 10,000 rpm for 5 minutes. The resulting supernatants were transferred to liquid chromatography (LC) vial for LC-qTOF-MS analysis.

LC-qTOF-MS conditions

The liquid chromatography-high resolution mass spectrometric system consisted of Shimadzu CBM-20A HPLC pump controller (Shimadzu Corporation, Columbia, MD, USA), 2 Shimadzu LC-20AD pumps, CTC HTS PAL autosampler (LEAP Technologies, Carrboro, NC, USA), and quadrupole time-of-flight (qTOF) TripleTOF™ 5600 mass spectrometer (Sciex, Foster City, CA, USA). The HPLC analytical column used was a C18 column 2.1 × 50 mm (Phenomenex, Torrance, CA, USA). The mobile phase consisted of: mobile phase A, distilled and deionized water containing 0.1% formic acid; and mobile phase B, acetonitrile containing 0.1% formic acid. The gradient was as follows: from 0 to 0.5 minutes, 10% B; from 0.5 to 0.9 minutes by a linear gradient from 10% B to 95% B; 95% B was maintained for 0.6 minutes; from 1.5 to 1.6 minutes by a linear gradient from 95% B to 10% B, and then 10% B was maintained for 1.4 minutes for column re-equilibrium. The gradient was delivered at a flow rate of 0.4 mL/min and the injection volume was 10 μL.

The TOF-MS scan mass spectra and the product ion scan mass spectra were recorded in the positive ion mode. The scan range was m/z 100–600 for both TOF-MS scan and product ion scan. For the quantification, $[M + H]^+$ ion of carisbamate and ISTD (m/z 216.0 and 455.3, respectively) were selected and their product ions at m/z 155.0 and 165.1 were used for quantitative analysis, respectively. The source temperature was set at 500°C with a curtain gas flow of 33 L/min. The ion spray voltage was set at 5,500 V. For Carisbamate and ISTD, declustering potential was 80 and 125 V, and the collision energy was 17 and 30 V, respectively.

Method qualification

The method qualification was performed with a 'fit-for-purpose' approach. The qualification run contained duplicate standards at seven concentrations and QCs at three concentrations. The acceptance criteria for standards and QCs in the qualification run were within ± 25% of the precision and accuracy values. A quadratic regression with an equation $y = ax^2 + bx + c$ was used to fit calibration curves over the concentration range for carisbamate. The accuracy and precision were calculated at each QC level concentration.

https://doi.org/10.12793/tcp.2020.28.e15

Extraction efficiency of carisbamate was also assessed using the same QC samples. The ratio of the mean concentration of pre-extracted spiked plasma to that of the blank plasma extracts spiked after extraction at the same concentration was used to calculate the extraction efficiency.

Preliminary stability assessments were performed to evaluate the different stability conditions; stock solution, short-term, long-term and freeze-thaw using low, medium and high QC samples. For stock solution stability assessment, prepared stock solution was stored at −20°C for 28 days. The short-term stability samples were stored at room temperature for 6 hours and long-term stability samples were kept frozen at −20°C for 28 days. For the freeze-thaw stability assessment, the samples were subjected to three freeze and thaw cycles at −20°C. The acceptance criteria for all stability tests were within ± 25% of the precision and accuracy values.

In vitro experiments

Plasma protein binding

The plasma protein binding assessment was carried out by equilibrium dialysis method in pooled SD rat and human plasma, respectively. The Thermo Scientific™ Rapid Equilibrium Dialysis device system (Thermo Scientific) was used for the equilibrium dialysis method. For the equilibrium dialysis, 300 µL of plasma samples containing carisbamate (1 µg/mL) were spiked into one insert and 500 µL of phosphate-buffered saline (PBS) was spike into the other insert, followed by equilibrium dialysis reaction for 4 hours at 37°C. After 4 hours, 100 µL of plasma samples was transferred to cluster tubes, and the same volume of PBS was added. In the same way, 100 µL of PBS samples was transferred to cluster tubes, and the same volume of blank plasma was added to make the same matrix conditions. Then, all samples were treated with the protein precipitation followed by the LC-qTOF-MS analysis. The unbound fraction of carisbamate in plasma (F_{up}) was obtained by the following formula:

$$F_{UP} = \left(\frac{Cu}{Ct}\right) * 100$$

In the above formula, Cu is the post-dialysis drug concentration in plasma, Ct is the post-dialysis drug concentration in PBS, which means the final concentration of unbound.

Microsomal metabolic stability

The microsomal metabolic stability in rat and human liver microsomes was investigated under the following final incubation conditions: carisbamate (0.2 µg/mL), rat and human liver microsomes (0.5 mg/mL) with β-nicotinamide adenine dinucleotide hydrate (NADPH) regenerating system solution (solution A is comprised of $NADP^+$ and glucose-6-phosphate [Glc-6-PO_4], while solution B is comprised of glucose-6-phosphate dehydrogenase [G6PDH]). First, a 5 minutes pre-incubation (37°C) was conducted by adding cofactor solutions containing NADPH regenerating system solution A & B to the liver microsomes. After pre-incubation, carisbamate was added to the liver microsomes suspension. All incubations were quenched with ACN containing ISTD at 0, 30, 60, and 120 minutes after incubation. Then, all samples were centrifuged and the each supernatant was analyzed by the LC-qTOF-MS method.

The *in vitro* intrinsic clearance, $CL_{int,\ in\ vitro}$ (mL/min/mg), was calculated by using the slope (k) of the log-linear regression analysis of the remaining % (the ratio of sample peak area/

https://doi.org/10.12793/tcp.2020.28.e15

ISTD peak area) versus time profiles, and The *in vivo* intrinsic clearance, CL_{int} (mL/min/kg), was calculated by scaling the *in vitro* values to the *in vivo* ones for rats and human by using following equation.

$$CL_{int,in\ vitro} = (slope\ k) * \left(\frac{mL\ microsomal\ volume}{mg\ microsomal\ protein}\right)$$

$$CL_{int} = CL_{int,in\ vitro} * \left(\frac{mg\ microsomal\ protein}{g\ liver}\right) * \left(\frac{g\ liver}{kg\ body}\right)$$

Where the liver microsomal protein concentrations were 44.8 and 48.8 mg microsomal protein/g liver in rats and humans, respectively, and the liver concentrations were 40 and 25.7 g liver/kg body weight in rats and humans, respectively [25]. The hepatic clearance (CL_H) extrapolated from CL_{int} using "well stirred" model is expressed as shown in equation below [26,27]:

$$CL_H = \left(\frac{Q_h * CL_{int}}{Q_h + CL_{int}}\right)$$

Where Q_h values, the hepatic blood flow, were 55.2 and 20.7 mL/min/kg in rats and humans, respectively.

Through "well-stirred" model, it was assumed that the liver was a well-stirred compartment and distribution equilibrium was achieved so quickly that the amount in the blood and the unbound amount in the liver were in equilibrium.

Application for a PK study in rat

All animal studies were performed in accordance with the "Guidelines in Use of Animal" established by the Chungnam National University Institutional Animal Care and Use Committee (Daejeon, Korea). This study was approved by the Chungnam National University Institutional Animal Care and Use Committee (No. CNU-01104). PK studies were conducted in SD rats (300 ± 10 g). All rats were fasted 12 hours prior to carisbamate administration. And then, carisbamate was administered to rats via intravenous bolus (IV) injection (1 and 2 mg/kg) or oral (PO) dose (1 and 5 mg/kg). The blood sampling time were 0, 2, 5, 10, 30, 60, 90, 120, 240, 360, and 1,440 min for IV PK and 0, 5, 15, 30, 60, 90, 120, 240, 360, and 1,440 minutes for PO PK in collection tube containing sodium heparin as anti-coagulant. Blood samples were centrifuged at 10,000 rpm for 5 minutes and supernatant plasma samples were stored at −20°C until analysis.

PK parameter estimates from IV or PO plasma concentration-time data were acquired using WinNonlin® version 8.0.0 (Certara, Princeton, NJ, USA). The nominal dose administered to each group was used to calculate PK parameters. PK parameters were calculated by non-compartmental analysis (NCA).

Prediction of PK profiles using the PBPK model

GastroPlus™ (version 9.7; Simulations Plus, Inc., Lancaster, CA, USA) PBPK model was used to predict the plasma concentration-time profile of rats and humans. In this study, the PBPK model was adopted as a perfusion-limited tissue model, which the kinetics of drug to tissue were determined by the Kp values (distribution coefficient).

https://doi.org/10.12793/tcp.2020.28.e15

Translational and Clinical Pharmacology TCP

Table 1. Input parameters used in GastroPlus™ for PBPK model simulation of carisbamate

Parameters	Values
Molecular weight (g/moL)	215.64
pKa*	11.98
LogP*	1.05
Permeability (cm^2/s)*	2.52
Solubility at pH 7 (mg/mL)*	6.66
Rbp in rat and human*	0.91
Unbound fraction (F_{up}) in rat and human (%)†	47.55 and 51.29
$CL_{int,\ in\ vitro}$ in rat and human (mL/min/kg)†	0.0009 and 0.0006

PBPK, physiologically based pharmacokinetic; Rbp, blood/plasma ratio.
All input parameters were calculated by GastroPlus™; *predicted values, †measured values.

In vitro data (unbound fraction in plasma and *in vitro* intrinsic clearance) were used as input parameters to build the PBPK model. GastroPlus™ ADMET predictor module was used for the prediction of physicochemical and ADME properties such as pKa, logP, permeability, solubility and blood/plasma ratio based on the structure of the carisbamate. The input parameters for PBPK simulation are summarized in **Table 1**. In addition to the *in vitro* data, PK parameters obtained by IV administration at a dose of 1 mg/kg in rats were used to optimize the PBPK model. The GastroPlus™ optimization module was used to optimize the PBPK model. The PBPK model was then validated using other *in vivo* PK data in rats and scaled to the PBPK model for human physiology. Then, human PK of carisbamate was simulated by population simulator (n = 12) using a scaled PBPK model, and the predicted PK results were compared with the observed baseline clinical data associated with food effect PK studies [7].

RESULTS

Method qualification

The calibration curves were selected based on the analysis of the data with weighted quadratic regression (1/concentration^2). The mean correlation coefficient (r) value was > 0.99 for the linearity of calibration curve ranged from 9.05 to 6,600 ng/mL. **Fig. 1** shows the calibration curve of carisbamate. Representative chromatograms of carisbamate (lower limit of quantification [LLOQ], 9.05 ng/mL) and verapamil (ISTD) samples are also shown in **Fig. 2**. The intra and inter-run accuracy and precision at 3 QC samples met the acceptance criteria of ± 25% and the results are shown in **Table 2**. The extraction efficiency of carisbamate was found to be 33.44% ± 2.47%. The protein precipitation method for sample preparation showed the robust recovery.

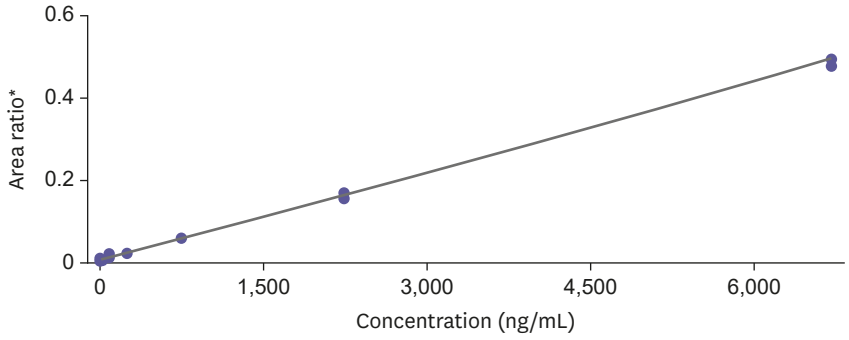

Figure 1. A calibration curve (r = 0.99156, range = 9.05–6,600 ng/mL) for carisbamate in rat plasma.
*Area ratio = Sample Peak Area/Internal Standard Peak Area.

https://doi.org/10.12793/tcp.2020.28.e15

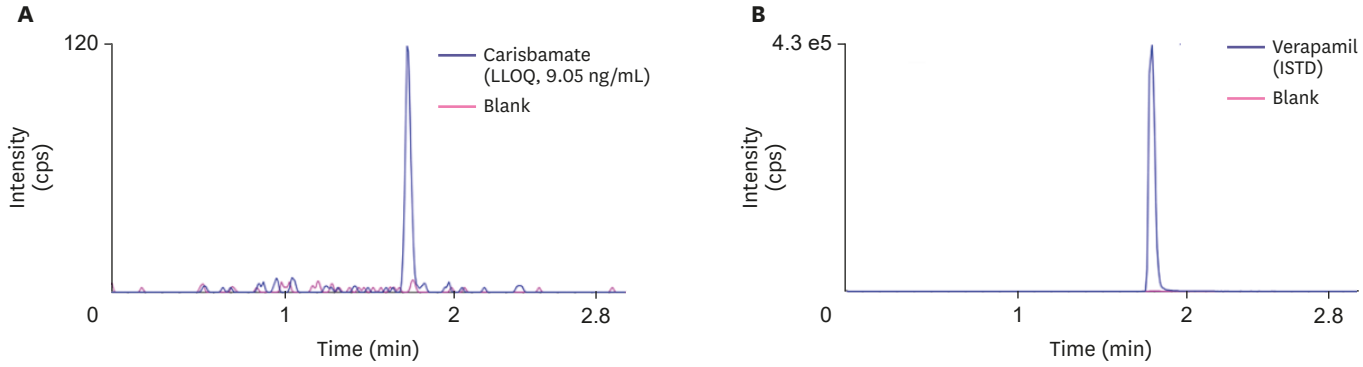

Figure 2. Typical chromatograms of carisbamate and verapamil. (A) LLOQ, 9.05 ng/mL of carisbamate, (B) verapamil (ISTD) with extracted blank matrix.
ISTD, internal standard; LLOQ, lower limit of quantification.

Table 2. QC results and statistics from the quantification run for carisbamate in rat plasma

Run No.	Statistics*	Low QC (15.04 ng/mL)	Medium QC (165.46 ng/mL)	High QC (1,820 ng/mL)
1	Mean	16.02	152.78	1,685.67
	% Acc	106.54	92.34	92.62
	% CV	12.03	0.90	6.29
	No. of samples	3	3	3
2	Mean	15.75	153.41	1,692.13
	% Acc	104.74	92.72	92.97
	% CV	8.35	3.07	5.35
	No. of samples	3	3	3
3	Mean	16.94	200.62	2,170.98
	% Acc	112.66	121.25	119.28
	% CV	9.77	3.73	3.77
	No. of samples	3	3	3
Inter-run	Mean	16.24	168.94	1,849.59
	% Acc	107.98	102.10	101.63
	% CV	9.42	14.31	13.75
	No. of samples	9	9	9

QC, quality control.
*Statistics calculate as follow: % Acc = accuracy % = (observed mean value/theoretical value) * 100; % CV = coefficient of variation = (standard deviation/mean) * 100.

Table 3. Preliminary stability test results for carisbamate in rat plasma

Assessment	Statistics*	Low QC (15.04 ng/mL)	Medium QC (165.46 ng/mL)	High QC (1,820 ng/mL)
Short-term (RT, 6 hours)	Mean	14.71	170.28	1,756.61
	% Acc	97.78	102.91	96.52
	% CV	18.57	6.46	5.52
	No. of samples	3	3	3
Long-term (–20°C, 28 days)	Mean	17.32	182.15	1,907.17
	% Acc	115.16	110.09	104.79
	% CV	4.87	5.53	1.84
	No. of samples	3	3	3
Freeze-thaw (–20°C, 3 cycles)	Mean	14.87	150.62	1,692.21
	% Acc	98.87	91.03	92.98
	% CV	17.66	3.30	2.25
	No. of samples	3	3	3
Stock (–20°C, 28 days)	Mean	18.18	172.78	1,890.50
	% Acc	120.86	104.43	103.87
	% CV	12.53	4.87	3.75
	No. of samples	3	3	3

QC, quality control; RT, room temperature.
*Statistics calculate as follow: % Acc = accuracy % = (observed mean value/theoretical value) * 100; % CV = coefficient of variation = (standard deviation/mean) * 100.

https://doi.org/10.12793/tcp.2020.28.e15

Table 4. The microsomal metabolic stability of carisbamate in rat and human liver microsomes

Species	$CL_{int,\ in\ vitro}$ (mL/min/mg)	CL_{int} (mL/min/kg)	CL_H (mL/min/kg)
Rat	0.0009 ± 0.0001	1.59 ± 0.10	1.54 ± 0.11
Human	0.0006 ± 0.0001	0.83 ± 0.11	0.76 ± 0.11

CL, clearance.

All the results of preliminary stability studies are shown in **Table 3**. As a results, the results indicated that carisbamate in rat plasma was stable for 6 hours at room temperature, which is sufficient enough for the sample preparation process, and stable for 28 days at −20°C, and also stable for 3 cycles of freeze-thaw process at −20°C. Also, carisbamate in stock solution was stable for 28 days at −20°C.

Generally, a LC-MS/MS method was applied to quantify small molecule drugs in bioanalytical samples because of sensitivity. However, due to the recent development of MS application technology, a LC-qTOF-MS also shows sufficient sensitivity to analyze bioanalytical samples, and many applications are applied in the references [28-31]. In addition, high resolution-full scan analysis using LC-qTOF-MS also can give us better picture of the metabolite profiles of the target compound. Therefore, the LC-qTOF-MS method was sufficient to develop and qualify for the bioanalysis of carisbamate in rat plasma.

In vitro experiments

As results of plasma protein binding test for carisbamate, F_{up} values were 47.55% and 51.29% in rat and human plasma, respectively. And the results of the microsomal metabolic stability in rat and human liver microsomes are shown in **Table 4**. $CL_{int,\ in\ vitro}$ values were 0.0009 and 0.0006 mL/min/mg microsomal protein in rat and human liver microsomes, respectively. The scaled CL_{int} values were 1.70 and 0.72 mL/min/kg, and the extrapolated hepatic clearance values were 1.65 and 0.70 mL/min/kg in rat and human, respectively. These F_{up} and $CL_{int,\ in\ vitro}$ values were used as input parameters for each species in Gastroplus™ (**Table 1**).

Application for a PK study in rat

The qualified LC-qTOF-MS method was successfully applied to a pharmacokinetic study of carisbamate in rats. **Fig. 3** shows the pharmacokinetic profiles of carisbamate after IV and PO administration in rats. PK parameters were calculated by NCA using Phoenix WinNonlin® and shown in **Table 5**. The results show that maximum plasma concentration (C_{max}) and area under the curve (AUC) was dose proportional, while clearance (CL) and volume of distribution (Vd) are dose-independent in both IV and PO at dose range of 1 to 5 mg/kg, so that carisbamate has a linear PK in this dose range. The average value of CL was about 3.98 mL/min/kg, indicating that the drug was very stable *in vivo* metabolic condition. The average of bioavailability (BA) was about 100%. It is assumed that the there is less concern of first-pass effect (FPE) or drug absorption for carisbamate in rats.

Table 5. Pharmacokinetic parameters of carisbamate after IV and PO administration at a dose range of 1 to 5 mg/kg in rats

Administration route	Dose (mg/kg)	No. of samples	$T_{1/2}$ (min)	T_{max} (min)	C_{max} (ng/mL)	AUC_{last} (ng*min/mL)	AUC_{INF} (ng*min/mL)	CL (mL/min/kg)	Vd (L/kg)
IV	1	3	315.22 ± 141.6	2.0 ± 0	1,262.02 ± 130.34	238,526.86 ± 51,457.51	252,189.38 ± 69,371.79	4.16 ± 1.07	1.56 ± 0.18
	2	3	265.75 ± 58.90	4.7 ± 4.62	2,091.42 ± 549.22	570,764.08 ± 235,907.17	587,742.97 ± 256,854.93	3.8 ± 1.37	1.24 ± 0.21
PO	1	4	336.74 ± 88.43	22.5 ± 10.61	580.42 ± 20.31	320,885.36 ± 30,274.45	338,124.98 ± 18,991.18		
	5	3	276.81 ± 23.26	40.0 ± 17.32	3,660.12 ± 681.66	1,636,689.10 ± 183,116.71	1,681,244.93 ± 197,618.19		

IV, intravenous bolus; PO, oral; $T_{1/2}$, half-life; T_{max}, time to maximum plasma concentration; C_{max}, maximum plasma concentration; AUC_{last} = area under the curve from 0 to last measurable time; AUC_{INF}, area under the curve from 0 to infinity; CL, clearance; Vd, volume of distribution.

https://doi.org/10.12793/tcp.2020.28.e15

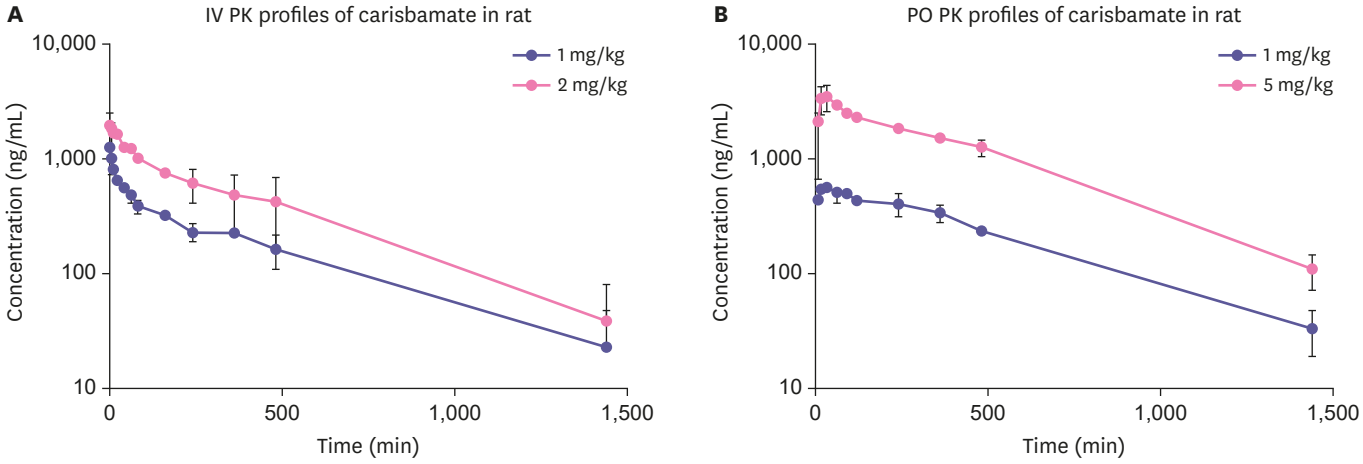

Figure 3. Time-concentration profiles of carisbamate after (A) IV administration at a dose of 1 and 2 mg/kg, (B) PO administration at a dose of 1 and 5 mg/kg.
IV, intravenous bolus; PO, oral; PK, pharmacokinetic.

Prediction of PK profiles using the PBPK model

The predicted and observed time-concentration profiles of carisbamate after a single IV administration at a dose of 1 mg/kg in rats are presented in **Fig. 4**. The first simulation was conducted using the input parameters only in **Table 1** and it showed an over-estimated result at the initial time point and under-estimated result at the later time point compared to the observed *in vivo* data (**Fig. 4A**). It was expected that the discrepancy between the predicted and the measured PK profile was due to the difference between the predicted and the measured Vd values. The liver and kidney are mainly considered to be organs that determine the disposition of small molecule drug [19,20]. In case of carisbamate, the previous studies show little metabolic disposition in the kidney [24,32,33]. Therefore, we assumed that carisbamate is primarily distributed and metabolized to liver. Based on this information, we optimized the liver Kp value to correct the difference between the predicted and the observed Vd value. GastroPlus™ optimization module was conducted for this optimization process. The predicted PK profiles in the PBPK model optimized for the Vd values were more similar to the observed PK profiles (**Fig. 4B**). The optimized PBPK model was then validated with other *in vivo* PK data and the results are shown in **Fig. 5**. **Fig. 5** shows that the optimized PBPK

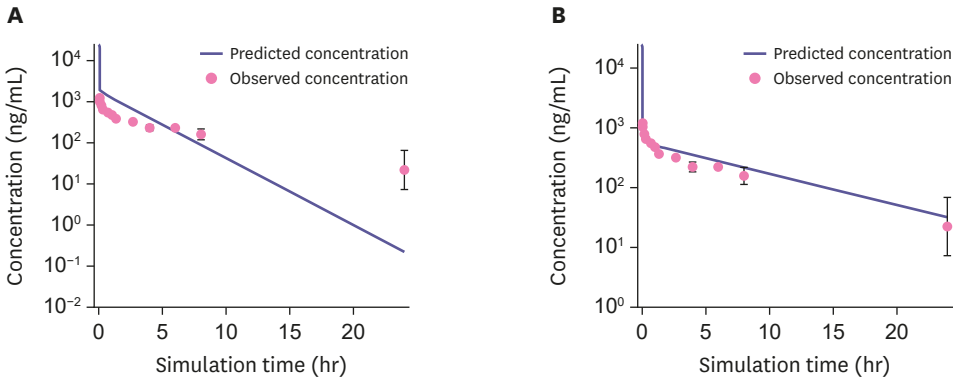

Figure 4. Predicted and observed time-concentration profiles of carisbamate after a single intravenous administration at a dose of 1 mg/kg in rats. (A) PK profile predicted only using the input parameters in **Table 1**, (B) PK profile predicted after optimizing the Kp value of liver.
PK, pharmacokinetic.

https://doi.org/10.12793/tcp.2020.28.e15

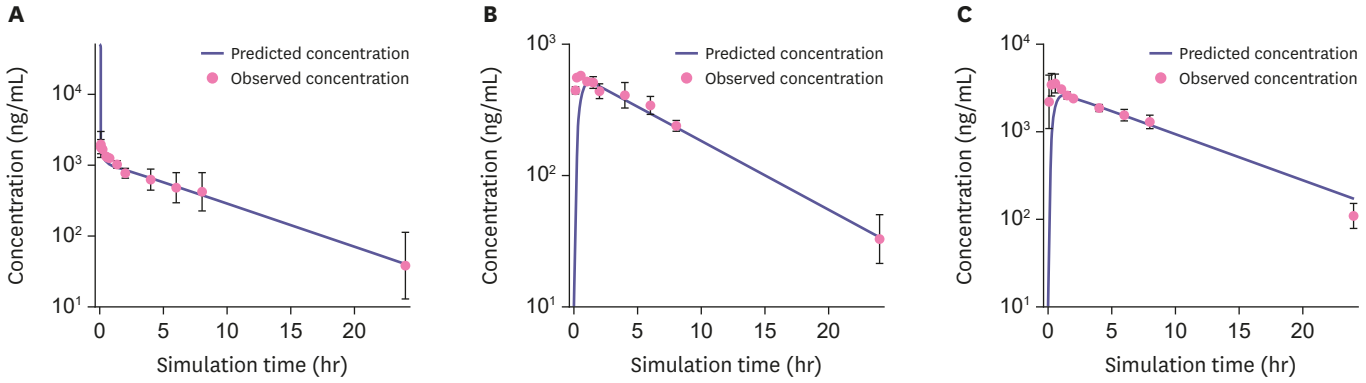

Figure 5. Predicted and observed time-concentration profiles of carisbamate after optimization, (A) intravenous administration at a dose of 2 mg/kg (B) oral administration at a dose of 1 mg/kg (C) oral administration at a dose of 5 mg/kg in rats.

Table 6. Population simulation and observed PK parameters of carisbamate at a dose of 750 mg in humans under fasted and fed conditions (each of n = 12)

PK parameters	Fasted condition				Fed condition			
	AUC_{last} (μg*hr/mL)	C_{max} (μg/mL)	T_{max} (hr)	$T_{1/2}$ (hr)	AUC_{last} (μg*h/mL)	C_{max} (μg/mL)	T_{max} (hr)	$T_{1/2}$ (hr)
Observed	199.7	11.8	1.9	13.1	190.4	10.5	3.4	12.9
Predicted	242.2	9.4	2.1	11.7	165.8	9.8	3.7	11.7
Prediction fold error	1.2	0.8	1.1	0.9	0.9	0.9	1.1	0.9

Prediction fold error are also included.
PK, pharmacokinetic; AUC_{last}, area under the curve from 0 to last measurable time; C_{max}, maximum plasma concentration; T_{max}, time to maximum plasma concentration; $T_{1/2}$, half-life.

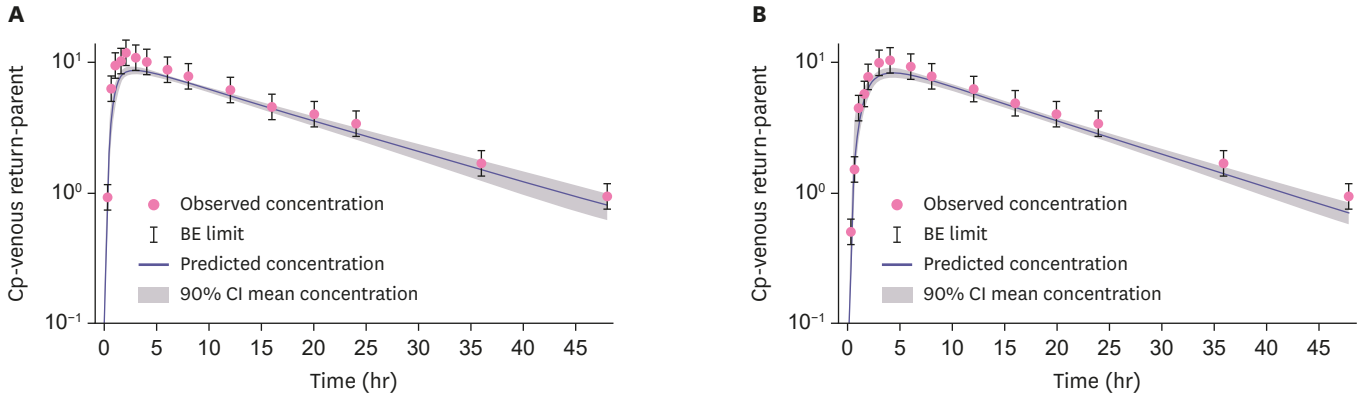

Figure 6. Population simulation and observed time-concentration profiles under after oral administration at a dose of 750 mg in humans under (A) fasted and (B) fed condition (each of n = 12).
BE limit, bioequivalence limit of observed concentration (80%–125%); 90% CI mean concentration, 90% confidence interval of predicted concentration.

model was well fitted when comparing the predicted PK profile with the observed PK profile at a different dose (2 mg/kg) or a different route of administration (oral administration). And then, the validated PBPK model by observed data in rats was scaled to human species. The human PK data orally administered at dose of 750 mg under physiologically fasted and fed condition were simulated by population simulator (n = 12) using scaled human PBPK model and compared to reference clinical data. The results are shown in **Fig. 6** and **Table 6**.

As a result, prediction fold error value was within 2 folds between the predicted and the reference clinical data in both fasted and fed conditions, suggesting that the predicted human PK profile and parameters are considerably acceptable from the industrial perspective [16,19,20,34].

https://doi.org/10.12793/tcp.2020.28.e15

DISCUSSION

In this study, an LC-qTOF-MS method was developed and qualified for the quantification of carisbamate in rat plasma. The calibration curve was acceptable over the concentration range from 9.05 to 6,600 ng/mL for carisbamate using quadratic regression with 1/concentration^2 weighting. This LC-qTOF-MS method was sensitive, selective, accurate and reproducible for the determination of carisbamate concentration and has been successfully applied to various *in vitro* and *in vivo* PK studies in rats. Several *in vitro* experiments and *in vivo* PK studies from preclinical species were used to successfully built a PBPK model and applied to predict the PK of carisbamate in humans. Overall, The optimized and validated PBPK model reasonably predicted the PK profile and the parameters of carisbamate in clinical PK study.

In conclusion, this study might indicate that the human PK prediction of carisbamate through PBPK modeling using *in vitro* data and *in vivo* data from preclinical species is expected to be a useful way to reduce time and cost associated with food effect studies and other various human clinical trials.

REFERENCES

1. Zannikos P, Novak G, Yao C, Verhaeghe T, Franc MA, Solanki B, et al. Pharmacokinetics of carisbamate (RWJ-333369) in healthy Japanese and Western subjects. Epilepsia 2009;50:1850-1859.
PUBMED | CROSSREF
2. Chien S, Yao C, Mertens A, Verhaeghe T, Solanki B, Doose DR, et al. An interaction study between the new antiepileptic and CNS drug carisbamate (RWJ-333369) and lamotrigine and valproic acid. Epilepsia 2007;48:1328-1338.
PUBMED | CROSSREF
3. Bialer M. The pharmacokinetics and interactions of new antiepileptic drugs: an overview. Ther Drug Monit 2005;27:722-726.
PUBMED | CROSSREF
4. Gonzalez M, Zannikos P, DiBernardo A, Brashear HR, Ariyawansa J. Effect of carisbamate on the pharmacokinetics and pharmacodynamics of warfarin in healthy participants. J Clin Pharmacol 2012;52:1420-1429.
PUBMED | CROSSREF
5. Moore K, Zannikos P, Solanki B, Greenspan A, Verhaeghe T, Brashear HR. Effect of mild and moderate hepatic impairment on the pharmacokinetics and safety of carisbamate. J Clin Pharmacol 2012;52:738-746.
PUBMED | CROSSREF
6. Trenité DG, French JA, Hirsch E, Macher JP, Meyer BU, Grosse PA, et al. Evaluation of carisbamate, a novel antiepileptic drug, in photosensitive patients: an exploratory, placebo-controlled study. Epilepsy Res 2007;74:193-200.
PUBMED | CROSSREF
7. Yao C, Doose DR, Novak G, Bialer M. Pharmacokinetics of the new antiepileptic and CNS drug RWJ-333369 following single and multiple dosing to humans. Epilepsia 2006;47:1822-1829.
PUBMED | CROSSREF
8. Kaur H, Kumar B, Medhi B. Antiepileptic drugs in development pipeline: a recent update. eNeurologicalSci 2016;4:42-51.
PUBMED | CROSSREF
9. Faught E, Holmes GL, Rosenfeld WE, Novak G, Neto W, Greenspan A, et al. Randomized, controlled, dose-ranging trial of carisbamate for partial-onset seizures. Neurology 2008;71:1586-1593.
PUBMED | CROSSREF
10. Novak GP, Kelley M, Zannikos P, Klein B. Carisbamate (RWJ-333369). Neurotherapeutics 2007;4:106-109.
PUBMED | CROSSREF
11. Halford JJ, Ben-Menachem E, Kwan P, Ness S, Schmitt J, Eerdekens M, et al. A randomized, double-blind, placebo-controlled study of the efficacy, safety, and tolerability of adjunctive carisbamate treatment in patients with partial-onset seizures. Epilepsia 2011;52:816-825.
PUBMED | CROSSREF

12. Sperling MR, Greenspan A, Cramer JA, Kwan P, Kälviäinen R, Halford JJ, et al. Carisbamate as adjunctive treatment of partial onset seizures in adults in two randomized, placebo-controlled trials. Epilepsia 2010;51:333-343.
PUBMED | CROSSREF

13. Yang F, Wang B, Liu Z, Xia X, Wang W, Yin D, et al. Prediction of a therapeutic dose for buagafuran, a potent anxiolytic agent by physiologically based pharmacokinetic/pharmacodynamic modeling starting from pharmacokinetics in rats and human. Front Pharmacol 2017;8:683.
PUBMED | CROSSREF

14. Allan G, Davis J, Dickins M, Gardner I, Jenkins T, Jones H, et al. Pre-clinical pharmacokinetics of UK-453,061, a novel non-nucleoside reverse transcriptase inhibitor (NNRTI), and use of in silico physiologically based prediction tools to predict the oral pharmacokinetics of UK-453,061 in man. Xenobiotica 2008;38:620-640.
PUBMED | CROSSREF

15. Brochot A, Zamacona M, Stockis A. Physiologically based pharmacokinetic/pharmacodynamic animal-to-man prediction of therapeutic dose in a model of epilepsy. Basic Clin Pharmacol Toxicol 2010;106:256-262.
PUBMED | CROSSREF

16. Bungay PJ, Tweedy S, Howe DC, Gibson KR, Jones HM, Mount NM. Preclinical and clinical pharmacokinetics of PF-02413873, a nonsteroidal progesterone receptor antagonist. Drug Metab Dispos 2011;39:1396-1405.
PUBMED | CROSSREF

17. De Buck SS, Sinha VK, Fenu LA, Nijsen MJ, Mackie CE, Gilissen RA. Prediction of human pharmacokinetics using physiologically based modeling: a retrospective analysis of 26 clinically tested drugs. Drug Metab Dispos 2007;35:1766-1780.
PUBMED | CROSSREF

18. Jones HM, Parrott N, Jorga K, Lavé T. A novel strategy for physiologically based predictions of human pharmacokinetics. Clin Pharmacokinet 2006;45:511-542.
PUBMED | CROSSREF

19. Wang B, Liu Z, Li D, Yang S, Hu J, Chen H, et al. Application of physiologically based pharmacokinetic modeling in the prediction of pharmacokinetics of bicyclol controlled-release formulation in human. Eur J Pharm Sci 2015;77:265-272.
PUBMED | CROSSREF

20. Gao ZW, Zhu YT, Yu MM, Zan B, Liu J, Zhang YF, et al. Preclinical pharmacokinetics of TPN729MA, a novel PDE5 inhibitor, and prediction of its human pharmacokinetics using a PBPK model. Acta Pharmacol Sin 2015;36:1528-1536.
PUBMED | CROSSREF

21. Lee BI, Park MH, Shin SH, Byeon JJ, Park Y, Kim N, et al. Quantitative analysis of tozadenant using liquid chromatography-mass spectrometric method in rat plasma and its human pharmacokinetics prediction using physiologically based pharmacokinetic modeling. Molecules 2019;24:1295.
PUBMED | CROSSREF

22. Miller NA, Reddy MB, Heikkinen AT, Lukacova V, Parrott N. Physiologically based pharmacokinetic modelling for first-in-human predictions: an updated model building strategy illustrated with challenging industry case studies. Clin Pharmacokinet 2019;58:727-746.
PUBMED | CROSSREF

23. Jones HM, Chen Y, Gibson C, Heimbach T, Parrott N, Peters SA, et al. Physiologically based pharmacokinetic modeling in drug discovery and development: a pharmaceutical industry perspective. Clin Pharmacol Ther 2015;97:247-262.
PUBMED | CROSSREF

24. Shardlow CE, Generaux GT, Patel AH, Tai G, Tran T, Bloomer JC. Impact of physiologically based pharmacokinetic modeling and simulation in drug development. Drug Metab Dispos 2013;41:1994-2003.
PUBMED | CROSSREF

25. Naritomi Y, Terashita S, Kimura S, Suzuki A, Kagayama A, Sugiyama Y. Prediction of human hepatic clearance from *in vivo* animal experiments and *in vitro* metabolic studies with liver microsomes from animals and humans. Drug Metab Dispos 2001;29:1316-1324.
PUBMED

26. Obach RS. Nonspecific binding to microsomes: impact on scale-up of *in vitro* intrinsic clearance to hepatic clearance as assessed through examination of warfarin, imipramine, and propranolol. Drug Metab Dispos 1997;25:1359-1369.
PUBMED

27. Obach RS. Prediction of human clearance of twenty-nine drugs from hepatic microsomal intrinsic clearance data: an examination of *in vitro* half-life approach and nonspecific binding to microsomes. Drug Metab Dispos 1999;27:1350-1359.
PUBMED

28. Fachi MM, Cerqueira LB, Leonart LP, Francisco TM, Pontarolo R. Simultaneous quantification of antidiabetic agents in human plasma by a UPLC–QToF-MS method. PLoS One 2016;11:e0167107.
PUBMED | CROSSREF

29. Paul D, Allakonda L, Satheeshkumar N. A validated UHPLC-QTOF-MS method for quantification of metformin and teneligliptin in rat plasma: application to pharmacokinetic interaction study. J Pharm Biomed Anal 2017;143:1-8.
PUBMED | CROSSREF

30. Lee BI, Park MH, Choi J, Shin SH, Byeon JJ, Park Y, et al. Liquid chromatography-high resolution mass spectrometric method for the quantification of monomethyl auristatin E (MMAE) and its preclinical pharmacokinetics. Biomed Chromatogr 2020;34:e4855.
PUBMED | CROSSREF

31. Park Y, Park MH, Byeon JJ, Shin SH, Lee BI, Choi JM, et al. Assessment of pharmacokinetics and metabolism profiles of SCH 58261 in rats using liquid chromatography-mass spectrometric method. Molecules 2020;25:2209.
PUBMED | CROSSREF

32. Mamidi RN, Mannens G, Annaert P, Hendrickx J, Goris I, Bockx M, et al. Metabolism and excretion of RWJ-333369 [1,2-ethanediol, 1-(2-chlorophenyl)-, 2-carbamate, (S)-] in mice, rats, rabbits, and dogs. Drug Metab Dispos 2007;35:566-575.
PUBMED | CROSSREF

33. Mannens GS, Hendrickx J, Janssen CG, Chien S, Van Hoof B, Verhaeghe T, et al. The absorption, metabolism, and excretion of the novel neuromodulator RWJ-333369 (1,2-ethanediol, [1-2-chlorophenyl]-, 2-carbamate, [S]-) in humans. Drug Metab Dispos 2007;35:554-565.
PUBMED | CROSSREF

34. Jones HM, Gardner IB, Watson KJ. Modelling and PBPK simulation in drug discovery. AAPS J 2009;11:155-166.
PUBMED | CROSSREF